URSI AP-RASC, Sydney, Australia, 17 – 22 August 2025

Combining RTK and TS to determine the position of array antenna of Mingantu Meter-Decameter Wavelength Spectral Radioheliograph of Chinese Meridian Phase II Project

Lihong Geng*(1), Linjie Chen (1), Wei Wang (1), Yihua Yan (1), Maosheng Yang (2), Donghao Liu (3), Zhichao Zhou (1), Jun Cheng (1), Cang Su (1)

(1) State Key Laboratory of Space Weather, National Space Science Center, CAS, 100190, Beijing, China

(2) Mingan Surveying and Mapping Company, Zhengxiangbaiqi, 013800, Inner Mongolia, China

(3) Key Laboratory for Exploration in the Moon and Deep Space, National Astronomical Observatories, CAS, 100101, Beijing, China

Abstract

The newly built MUSER-L of the Chinese Meridian Phase II Project, and the existing MUSER-I and MUSER-H, are all solar dedicated radioheliographs, based on the principle of synthetic aperture and utilizing array antennas for radio imaging observations. The position accuracy of these array antennas affects the accuracy of time delay compensation and phase compensation, which in turn affects the synthetic image quality. Methods and results of combining RTK and Total Station to determine the initial geometric position of array antennas of MUSER-L, as well as those of MUSER-I and MUSER-H are introduced.

1. Introduction

The Chinese second phase of the Meridian Project (hereinafter referred to as Meridian Project II) is funded by the National Development and Reform Commission of the People's Republic of China, and led by the National Space Science Center of the Chinese Academy of Sciences. The purpose is to establish a ground space environment monitoring system, forming a complete observation chain from the sun to the earth, providing more in-depth and extensive information on 49 key specifications of space environment for the study of space weather and solar physics. About 300 devices from 31 observation stations are arranged along latitude 30 ° and 40 ° N, longitude 100 ° and 120 ° E. The Meridian Project II also covers four regions including low latitude, mid latitude, Qinghai Tibet Plateau, and polar regions. Specific monitoring targets include the middle and upper atmosphere, ionosphere, geomagnetic field, and interplanetary space from the Sun to Earth. The Mingantu Observation Station in North China is one of the 31 stations that have built three sets of equipment for the Meridian Project II, including the Interstellar Scintillation Monitor (IPS), the Meter-Decameter Wavelength Radio Heliograph (MUSER-L), and the Ultra-Wideband Solar Radio Spectrometer (UWSRS). With the addition of 100 antennas from the two arrays of the previous centimeter-decimeter wavelength radioheliograph (MUSER-I and MUSER-H), the Mingantu Observatory currently has approximately 330 antennas. These antennas distributed in three spiral, five spiral, parallel, and circular ways on a 10 square kilometer grassland composing of a complex antenna configuration. Figure 1 shows the antenna layout at Mingantu Observing Station.

MUSER-L works on 30MHz-400MHz (the wavelength is 75cm-10m) with 2 linear polarizations. It has two antenna arrays of 124 stational Log Periodic Dipole Array (LPDA) antennas and 100 steerable LPDA antennas. The stational 124 LPDA antennas array is used as calibrator and spectrometer, and for multibeam imaging of the Sun, while the steerable 100 LPDA antennas array is dedicated for aperture synthetic imaging of the Sun at ~0.5-5 $R_\odot$. The position accuracy of these array antennas affects the accuracy of time delay compensation and phase compensation, which in turn affects the synthetic image quality. The antenna position accuracy requirement is mainly related to the operating wavelength of the equipment. The shorter the wavelength, the higher the position accuracy required. For MUSER-L and MUSER-I/H, this position accuracy requirement is at cm-level and mm-level. After measurements using the engineering methods of Total Station and RTK to get initial geometric antenna position, strong radio sources or synchronous orbit satellites need to be observed to obtain the final high-precision antenna position of MUSERs. Some other equipment such as NoRH, EOVSA, LOFAR and DART, more precise time delay and phase measurements rely on redundant baselines, observation of strong radio sources or synchronous orbit satellites with known precise positions, or high calibration towers.

Figure 1. Layout of array antenna at Mingantu Observing Station

2. Positioning the Structure Center of MUSER antennas by RTK and TS

Total Station (TS) method has high precision, requiring the establishment of a high-precision local control network, good ground intervisibility and good weather conditions. The deviation of control points will affect the TS measurement results, especially in long-distance measurements, where the accumulated error will be more pronounced. Compared to TS, Real Time Kinematic (RTK) method has slightly lower accuracy, based on Continuously Operating Reference Stations (CORS) network and service system, with reduced accuracy at a distance from CORS reference stations. Each RTK measurement is independent. The better visibility to the sky, more navigation satellite signal channels received and the stabler the Earth's ionospheric, the better RTK accuracy. Wide distribution range of antennas, undulating terrain, occlusion, complex layout, and lack of control points (many points spread on the 10 square km grassland of the control network built more ten years ago were damaged), increase the difficulty of determining high-precision geometric position of array antenna with one engineering method. Table 1 lists measurements of antenna arrays of MUSER-I, MUSER-H and MUSER-L. T1 and T2 were earlier measurements for MUSER-I and MUSER-H using TS based on 3-4 anchor bolts of antenna square structure foundation. R1 and R2 were two measurements using RTK based on 8-9 anchor bolts of the circular LPDA structure foundation of MUSER-L. T3 was a TS direct measurement of the antenna structure center before LPDA antennas of MUSER-L array were mounted. Due to intervisibility issues, T4, T5 and T6 were incomplete measurements using TS for MUSER-L, MUSER-I and MUSER-H separately based on several anchor bolts. Formula (1) gives computing method to obtain the circular structure center O_{mn} of LPDA antenna from bolts measurements M_i and designed structure radius in R1 and R2 surveying. In iterative calculations, points with large deviations are gradually removed, one example is showed in Figure 2. Figure 3 presents the similar process to obtain the square antenna structure center. Figure 4 gives the RMS of R2 in iterative calculations. The RMS with the last 5 points to positioning the center is better than 4mm.

Table 1. Measurements by TS and RTK on the 3-antenna array of MUSER-L, MUSER-I/H

Equipment	Identifier	Array	Antenna Number	Date
Total Station PENTAX-R202 Range accuracy: $\pm(2+2ppm\times D)mm$ Angle accuracy: 2"	T1	MUSER-I	40/40	2011 ~ 2012
	T2	MUSER-H	60/60	
RTK-ZHD V300 Positioning accuracy: Plane: $\pm(8+1ppm\times D)mm$ Altitude: $\pm(15+1ppm\times D)mm$	R1	MUSER-L	100/100	2023 Dec.~ 2024 Jan.
	R2	MUSER-L	100/100	2024 Jun.
Total Station SET220K Range accuracy: $\pm(2+2ppm\times D)mm$ Angle accuracy: 2"	T3	MUSER-L	100/100	2022 Oct. ~ 2023 Jul.
	T4	MUSER-L	76/100	2024 Oct. ~ 2024 Dec.
	T5	MUSER-I	29/40	
	T6	MUSER-H	41/60	

$$D_{mn} = \sqrt{\frac{1}{k}\sum_{i=1}^{k}(M_iO_{mn} - Radius)^2} \qquad (1).$$
$$D_{min} = min\,(D_{mn})$$

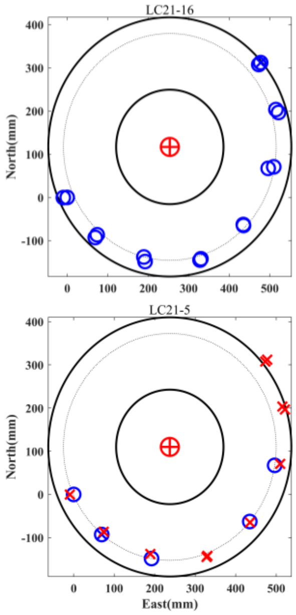

Figure 2. Computing the center of the circular structure foundation of LC21 of MUSER-L antenna array, for initial 16 points(up) and 5 points (bottom, with 11 points with large deviations have been removed) in R2 measurement.

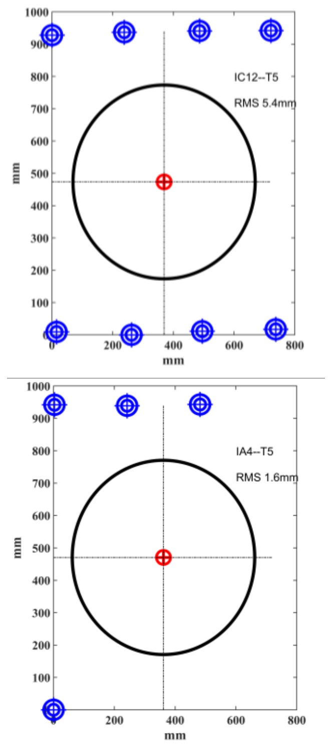

Figure 3. Computing the center of the square structure foundation of IC12 and IA4 of MUSER-I antenna array in T5 measurement.

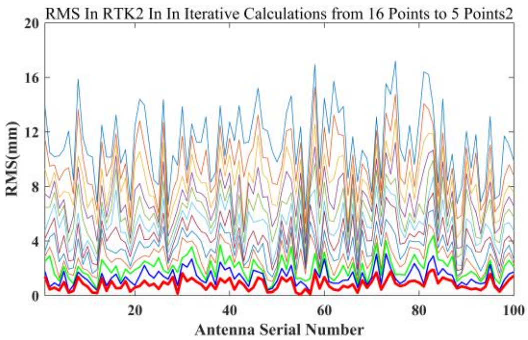

Figure 4. RMS of R2 in iterative calculations from 16 points to 5 with large deviations are gradually removed.

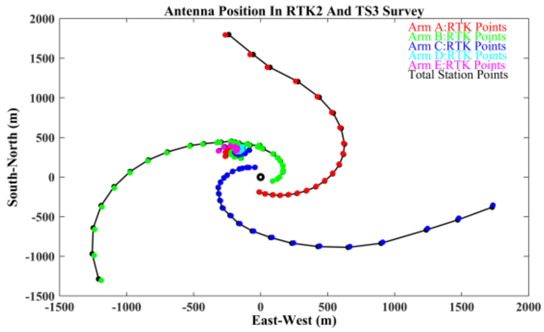

Figure 5. 100 LPDA positions of MUSER-L by R2 and T3.

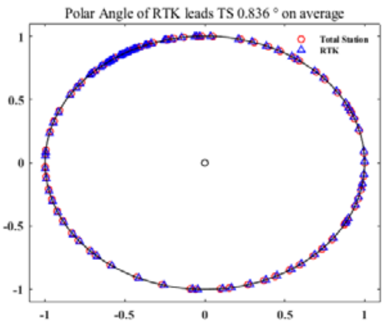

Figure 6. Polar angel of R2 leads T3 0.836° on average.

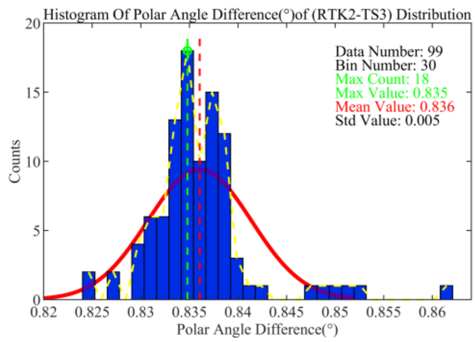

Figure 7. Histogram distribution of polar angel difference.

3. Unifying RTK and TS Coordinates Based on Statistical Method

The antenna positions from TS measurement are topocentric coordinates, with IA0 antenna of MUSER-I as the coordinate origin, east as axis Y positive and north as axis X positive. This north directs to the earth's rotation axis and was determined by observing the Polaris. In radioheliograph imaging process, topocentric coordinates is first changed into Geocentric coordinate, then changed into observing coordinate. The antenna positions from RTK measurements are NEZ plane coordinates, refers to the x-coordinate, y-coordinate, and normal height of the Gaussian projection plane Cartesian coordinate system, converted from CGCS2000 (China Geodetic Coordinate System 2000) Geocentric coordinate system. The geographic coordinates of Mingantu Observatory (115.15 ° E, 42.12 ° N) are far from the central meridian (114 °) of the 38th 3° zone in the Gaussian Kruger projection, and length deformation is inevitable. Observed data are compared among R2, R1 and T3 for outlier removal and statistical methods are used to obtain coordinates rotation coefficient and scale coefficient to unify R2 and T3. Figure 5 to Figure 9 present the data proceeding process.

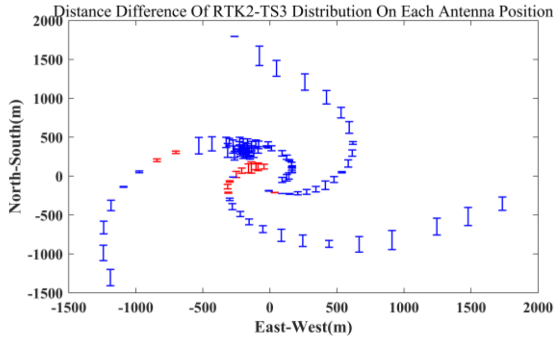

Figure 8. Position distribution of polar distance difference of R2 and T3.

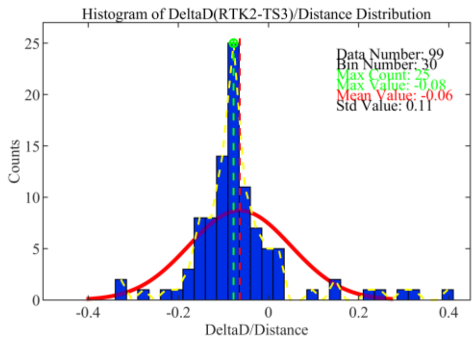

Figure 9. Histogram distribution of polar distance difference of R2 and T3.

4. Discussions and Conclusion

100 MUSER-L LPDA antenna positions have been measured and calibrated carefully. The solar imaging results show that MUSER-L is capable to make the daily solar observations and is capable to monitor and image the sun with high-temporal, high-spectral and high-spatial resolution. Figure 10 gives the preliminary solar radio images by MUSER-L on frequency of 58.5938 MHz, 160.1953 MHz and 326.0156 MHz (from top to bottom) on Oct. 24, 2024. Further work on MUSER-I and MUSER-H antenna positioning is underway.

5. Acknowledgements

This study is supported by the Chinese Meridian Project Phase II. We would like to thank Jianxi Ren, Sulide, Haibing and Gunter for their help in field measurements.

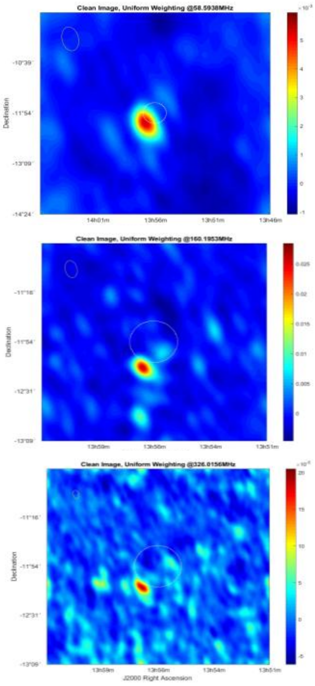

Figure 10. Preliminary Solar radio images by MUSER-L on frequency of 58.5938 MHz, 160.1953 MHz and 326.0156 MHz (from top to bottom) on Oct. 24, 2024.

References

[1] Yihua Yan, Zhijun Chen, Wei Wang, et al., "Mingantu Spectral Radioheliograph for Solar and Space Weather Studies," *frontiers in Astronomy and Space Sciences*, 29, March 2021, pp. 1-13, doi:10. 3389/fspas.2021.584043.

[2] Wang Chi, Xu Jiyao, Lu Daren, et al., "Construction Progress of Chinese Meridian Project Phase II," *Chin. J. Space Sci.*, 2022, **42**, 4, pp. 539-545, doi:10.11728 /cjss2022.04. yg09.

[3] Liu Donghao, Yan Yihua, Wang Wei, et al., "Baseline Measurement of the Antenna Array for the Chinese Spectral Radioheliograph in the Centimeter-to-Decameter Wave," *ASTRONOMICAL RESEARCH AND TECHNOLOGY*, 2013,**10**, 2, pp.128-133, Doi: 10. 3969/j.issn.1672-7673.2013.02.004.

[4] Liu Donghao, Yan Yihua, Zhao An, et al., "A Delay Calibration for Chinese Spectral Radioheliograph in the decametric to centimetric wave range," *ACTA ELECTRONICA SINICA*, 2013, **41**, 3, pp. 570-574, Doi: 10.3969/j.issn.0372-2112.2013.03.025.

[5] Liu Donghao, "Research on Calibration of the New Generation Centimeter-Decimeter Wave Radiohelio graph (CSRH) System," *Ph.D. dissertation*, National Astronomical Observatories, CAS, Apr. 2012.

[6] Thompson A R, J M Moran, G W Swenson, "Interferometry and synthesis in radio astronomy," New York: Wiley, 2001.

[7] Wang Wei, Yihua Yan, Liu Donghao, et al., "Phase Calibration Using Satellite as Calibrator for Mingantu Spectral Radioheliograph," *ACTA ELECTRONICA SINICA*, Jun, 2019, **47**, 6, pp.1384-1387, doi:10. 3969/j.issn.0372-2112.2019.06.028.

[8] Geng Lihong, Yihua Yan, Linjie Chen, et al., "Array antenna position measurement of Chinese Meridian Project Phase II at Mingantu Observing Station," *URSI GASS 2023*, Doi: 10.23919/URSIGASS57860. 2023.

[9] Geng Lihong, Yihua Yan, Linjie Chen, et al., "A RTK based array antenna positioning method of Chinese Meridian Project Phase II at Mingantu Observing Station,"*2024 4th URSI Atlantic Radio Science Meeting (AT-RASC)* ,Meloneras, Spain, 2024, pp. 1-3, Doi: 10.46620/URSIATRASC24/ULMZ6261.

[10] Hideki Koshiishi, Shinzo Enome, Hiroshi Nakajima, et al., "Evaluation of the Imaging Performance of the Nobeyama radioheliograph". *PASJ: Publ. Astron. Soc. Japan*, 46, L33-L36 (1994).

[11] Linjie Chen, Yihua Yan, Wei Wang, et al., "Meter to Decameter Wave Spectral Radio Heliograph," *2020 XXXIIIrd General Assembly and Scientific Symposium of the International Union of Radio Science*, Rome, Italy, 2020, pp. 1-4, doi: 10.23919/ URSIGASS49373.2020. 9231998.

[12] Linjie Chen, Wei Wang, Yihua Yan, et al., "Solar Radio Observations with Meter to Decameter Wave Spectral Radio Heliograph," *2024 4th URSI Atlantic Radio Science Meeting (AT-RASC)*, Meloneras, Spain, 2024, pp. 1-3, doi:10.46620/ URSIATRASC 24/ULMZ6261.

[13] Sebastiaan van der Tol, Brian D. Jeffs and Alle-Jan van der Veen, "Self-calibration for the LOFAR radio astronomical array," *IEEE Transactions on signal processing*, **55**, 9, pp. 4497-4510.

[14] Stefan J. Wijnholds, Sebastiaan van der Tol, Ronald Nijboer, et al., "Calibration Challenges for Future Radio Telescopes," *IEEE Signal Processing Magazine*, January 2010, **27**, 1, pp. 30-42, doi:10.11 09/MSP.2009.934853, Copyright IEEE.

[15] Guadalupe Esteban Bazquez Becerra, Rick A. Bennett, Mijaíl Cordero Chávez, et al., "Short Baseline Calibration using GPS and EDM observations," *Geofísica International*, 2015, **54**, 3, 255-266, doi:10.1016/j.gi.2015.04.017.

[16] S.V. Lesovoi, A.T. Altyntsev, A.A. Kochanov, et al., "Siberian Radioheliograph: First Results," *Solar-Terrestrial Physics*, 2017, **3**, 1, pp. 3–18, doi:10.1273 7/article_58f96ec60fec 52.86165286.

[17] A.Yu. Fedotova, A.T. Altyntsev, A.A. Kochanov, et al., "Calibration of Siberian Radioheliograph Images," *Solar-Terrestrial Physics*, 2019, **5**,4, pp. 27–33, doi: 10.12737/stp-54201904.

[18] Antenna Position-EOVSA Wiki (njit.edu). http:// ovsa.njit.edu//wiki/index.php?title=Antenna_Positio n&oldid=1504.

[19] Yang Yuanxing, "Selection and Computation of Projection Datum Plane with Compensation effect," *Urban Geotechnical Investigation & Surveying*, 2008, 2, pp.72-74